ISBN: 978-3-95450-247-9 ISSN: 2673-5490 doi: 10.18429/JACoW-IPAC2024-TUPS39

BENCHMARKING POWER DEPOSITION FROM FAST LOSSES OF HEAVY-ION BEAMS AT THE ONSET OF LHC RUN 3*

V. Rodin†, R. Bruce, R. Cai, M. D'Andrea, L. Esposito, A. Lechner, D. Mirarchi, S. Morales Vigo, S. Redaelli, B. Salvachua, P. Schoofs, CERN, Geneva Switzerland

Abstract

In 2023, the LHC started its Run 3 operation with $^{208}Pb^{82+}$ beams at 6.8 ZTeV, with a substantially higher number of bunches compared to past runs. Several new hardware systems were used operationally for the first time with high-intensity beams, including bent crystal collimators in the betatron cleaning insertion. Crystal-assisted collimation reduces the leakage of secondary ion fragments to the downstream dispersion suppressors, therefore decreasing the risk of quenching superconducting magnets. One of the limitations encountered during the 2023 run were events with fast beam losses impacting the collimation system, which triggered multiple premature beam aborts on Beam Loss Monitors (BLMs). In this contribution, we present energy deposition simulations for these events, performed with the FLUKA tool, aiming to quantify the quench margin for the fast loss regime (~30 ms). To assess the predictive ability of the model, benchmarks against 2023 measurements are presented. The studies provide an important input for fine-tuning BLM thresholds in future heavy-ion runs, therefore increasing the tolerance to beam losses and hence the LHC availability.

INTRODUCTION

In 2023, the LHC heavy-ion program with fully stripped lead ion beams ($^{208}Pb^{82+}$) beams was the first operational period with all High-LUminosity LHC (HL-LHC) ion upgrades in place. Numerous improvements were carried out within the LIU [1] and HL-LHC projects [2], allowing to reach beam intensities around 2×10^{11} ions [3]. In addition, the ion energy was raised from 6.37 *Z*TeV in Run 2 (2015-2018) to 6.8 *Z*TeV in 2023. The total stored beam energy reached 17.35 MJ in 2023, which was a significant increase compared to the 12.9 MJ previously achieved during Run 2. Such a stored energy poses a significant challenge for a superconducting machine like the LHC, where already beam losses of a few tens of mJ can quench magnets if the particles would be lost in an uncontrolled way. To mitigate the adverse effects of beam halo losses, the LHC accommodates a multi-stage collimation system [4, 5], which represents a global aperture bottleneck and intercepts beam particles before they are lost in magnets. Together with the Beam Loss Monitor (BLM) system [6], which continuously records beam losses and can trigger beam aborts in case of excessive losses, both systems function as a protective measure to avoid recurring quenches, which would significantly perturb the machine availability.

The collimation system consists of two main sub-systems located in different insertion regions (IRs), the betatron cleaning system in IR7 and the off-momentum cleaning system in IR3. Currently, the collimation system comprises more than 100 collimators for both beams. The betatron cleaning system in IR7 operates with a three-stage collimator hierarchy, consisting of primary and secondary collimators, as well as shower absorbers. Beam collimation is more challenging for heavy ions than for protons due to nuclear fragmentation and electromagnetic dissociation within the collimator material and the consecutive leakage of secondary fragments to downstream dispersion suppressor (DS) magnets [7]. In order to reduce the leakage to cold magnets, a new collimation technique based on bent crystals has been implemented operationally for the first time with high intensities in the 2023 ion run [8–10]. The crystals were used as primary collimators in the IR7 betatron cleaning system, deviating the beam halo through channeling (CH) on a secondary collimator [11, 12]. Previous experimental studies [13] and shower simulations [14–16] had shown that the power deposition in cold magnets downstream of IR7 can be reduced by a factor 7 compared to the standard system.

During the 2023 heavy-ion run, fast beam losses in the crystal-based system gave rise to tens of beam aborts by the BLMs. Although no quenches were observed, the recurring beam dumps still had an important impact on the machine performance due to reduced availability [17]. In many cases, the loss events had a multi-peak time structure, with a typical peak duration of tens of milliseconds. The time structure was

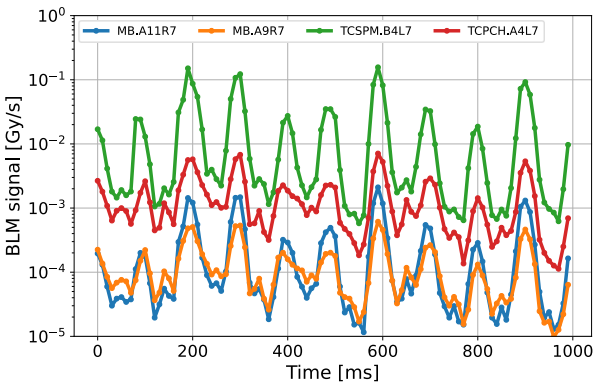

Figure 1: Example of fast beam loss spikes measured by different BLMs in the betatron cleaning insertion and the downstream dispersion suppressor during one heavy-ion fill in 2023. The repeating loss spikes are assumed to be caused by vibrations of a certain magnet.

* Research supported by the HL-LHC project.
† volodymyr.rodin@cern.ch

ISBN: 978-3-95450-247-9 ISSN: 2673-5490 doi: 10.18429/JACoW-IPAC2024-TUPS39

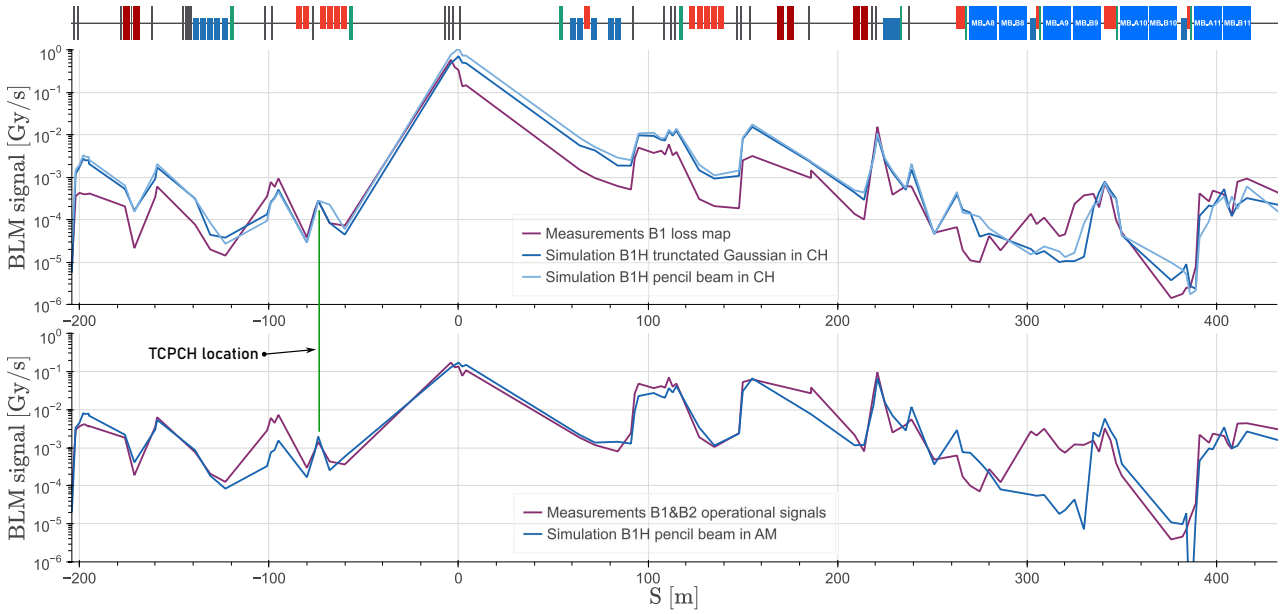

Figure 2: Simulated and measured BLM signals for heavy ion losses in IR7. The ion beam direction is from left to right. The two figures consider the cases that the horizontal crystal is in channeling (top) and in amorphous orientation (bottom). The measurements were recorded in the 2023 heavy ion run at 6.8 ZTeV. The crystal is located at around s=-75 m, whereas the secondary collimator intercepting the channeled beam is located at s=0 m.

possibly caused by the vibrations of a certain magnet, which lead to a fast modulation of halo losses. Figure 1 shows the signals from four BLMs for one such event (Fill 9291). The red line corresponds to the BLM located near the crystal collimator. In green is the signal from the BLM next to the secondary collimator, which intercepts the channelled beam. Comparable oscillations could also be observed on other BLMs in IR7, as well as at downstream cold magnets due to the leakage of fragments (blue and orange curves). Another factor contributing to the recurring beam dumps was an intermittent degradation of the halo cleaning efficiency due to a non-ideal angular alignment of the crystals. The misalignment was possibly caused by heating. In the worst case, if channeling conditions are lost, the crystal can act as an amorphous absorber, which leads to an enhanced leakage of fragments to cold magnets. In order to optimize the beam abort thresholds for future heavy-ion runs, it is essential to quantify the maximum allowed betatron halo loss rate for the millisecond time regime without quenching DS magnets. In this paper, we present FLUKA [18, 19] energy deposition studies for crystal-assisted collimation and compare the results with quench limits of DS dipoles. Contrary to previous energy deposition studies for crystal collimation [14–16], we give particular attention to fast losses and we also address the loss of channeling conditions. In order to validate our simulation model for the 2023 machine configuration, we first present benchmarks of simulated BLM signals against measurements from 2023 operation.

FLUKA BENCHMARK OF BLM SIGNALS

To accurately evaluate BLM signals and the power deposition inside magnet coils, collimator jaws and other equipment, a multi-step simulation chain was developed [20]. The initial step requires multi-turn tracking in SixTrack [21, 22], coupled with FLUKA, to realistically model interactions with collimators and crystals [23, 24]. The following simulation step is carried out with a stand-alone FLUKA model of the IR7 region, implementing magnetic fields based on the underlying optics. In order to quantify the energy deposition in different elements, the main geometrical features of collimators and magnets in the IR are accurately represented in the model. As source distribution, the second step uses the impact distributions of particles on the crystal and collimators obtained in the first step. More details on the complete simulation workflow can be found in Refs. [20, 25].

In order to perform a benchmark of simulated BLM signals against measurements from the 2023 ion run, the 2023 machine configuration (optics and collimator gaps) was implemented in the FLUKA model. The half-gaps of collimators are usually specified as the number of beam σ for a normalized transverse proton emittance of 3.5 μm rad. The crystal collimators for the vertical and horizontal planes (called TCPCV and TCPCH) were positioned at 4.75σ from the beam, while the standard primary collimators (TCPs) located further upstream were retracted to a larger half-gap of 6σ. The secondary collimators (TCSGs) and shower absorbers (TCLAs) were positioned at half-gaps of 6.5σ and 8σ, respectively.

As the initial source for the production of secondary showers and multi-turn losses, a pencil beam of $^{208}Pb^{82+}$ ions was assumed to hit the TCPCH crystal at a specific distance from its edge. The considered impact depth was 1 µm. The incident angle for the primary ions was matching the x' value at the defined x location in the horizontal phase space ellipse

ISBN: 978-3-95450-247-9 ISSN: 2673-5490 doi: 10.18429/JACoW-IPAC2024-TUPS39

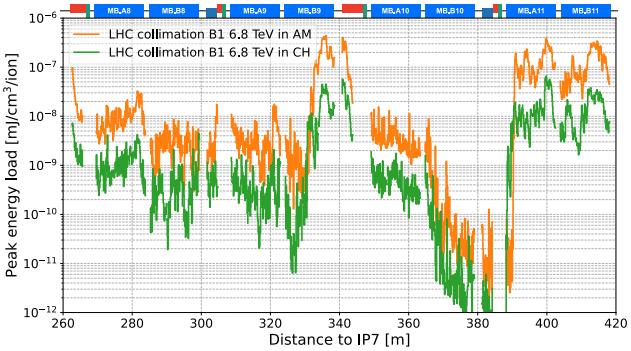

Figure 3: Expected peak energy deposition in the superconducting coils of DS magnets (MBs) next to IR7 (6.8 ZTeV $^{208}Pb^{82+}$). The two curves assume that the crystal is in channeling orientation (CH) and in amorphous orientation (AM).

at the crystal location. Only losses in the horizontal plane were modelled. The bending angle of the horizontal crystal was obtained from qualification X-ray measurements [13] and was set to 51 µrad.

Figure 2 shows a comparison of simulated and measured BLM signals in IR7 and in the DS region up to cell 11. Two scenarios were considered, one assuming that the TCPCH was in ideal channeling orientation (upper figure), and one assuming that the beam halo particles experience only amorphous interactions with the crystal (bottom figure). For the first scenario, a second FLUKA simulation was performed where the initial conditions were, instead of a pencil beam, a truncated Gaussian distribution with a lower limit of 4.75 σ. This modification helped to validate the pencil beam approach and provided a more conservative estimate of the channeling rate inside the crystal. In all cases, the simulation results were scaled to match the measured BLM signal at the secondary collimator, which acted as absorber for channeled ions.

A satisfactory agreement is found between simulated and measured signals for the channeling case. During the studied loss event, both beams were present inside the machine, but losses were artificially induced for one beam and plane only (horizontal plane of Beam 1). The largest discrepancy (overestimation by factor 5) is observed between s=0 m and 200 m, right after the secondary collimator which intercepts the channeled halo. The reasons for these discrepancies are under investigation, although agreement on the crystal and absorber collimator is excellent. Nevertheless, a good agreement (within a factor 2) is achieved for the maximum signal in the DS region, the main focus of our study.

An excellent agreement is observed for the case of amorphous interactions as depicted in the bottom graph of Fig. 1. The only difference compared to the channeling simulations was the deactivation of the channeling process in the FLUKA setup. Some discrepancy between simulation and measurement is observed around s=300 m, an issue we are investigating further.

ENERGY DEPOSITION IN DS MAGNETS

Using the same simulation model as in the previous section, we evaluated the maximum energy deposition density in magnet coils, in order to assess the maximum allowed ion loss rate in the collimation system without inducing a quench. Similarly to previous studies [14–16, 26], a three-dimensional cylindrical mesh was superimposed on the magnet coils for scoring the energy deposition. The longitudinal profile of the peak energy deposition density in dispersion suppressor magnets downstream of IR7 is shown in Fig. 3. As in the previous section, the figure presents results for Beam 1. The results are given per ion lost in the collimation system. The plot illustrates that in both cases, with the crystal in channeling and amorphous orientation, the highest energy density occurs in the main dipoles MB.B9 and MB.A11 located in half-cells 9 and 11, respectively. We also observe a similar level of energy deposition in one of the quadrupoles (MQ.10), which is however less likely to quench due to the higher quench margin [27]. The clear difference in amplitude between the orange and green curves distinctly highlights the increase of particle leakage in case the crystal acts as an amorphous absorber.

The quench margin of superconducting magnets in case of beam-induced heat deposition can be calculated by means of electro-thermal models. Assuming a loss duration of 10–30 ms and a beam energy of 6.8 ZTeV, the quench level of LHC main bending dipoles is predicted to be in the range between 65 mJ/cm^3 and 100 mJ/cm^3 [27, 28]. These theoretical estimates are also supported by observations made in Run 2 proton operation. Several loss events were observed in 2017, which induced an estimated energy density of about 50 mJ/cm^3 without triggering a quench [29]. These events had a different root cause (micrometer-sized particulates entering the beam), but the concerned magnet type (bending dipole) and the loss duration (tens of milliseconds) were the same as for the collimation losses discussed in this paper.

Considering the lower bound predicted by the electro-thermal models (65 mJ/cm^3) and taking into account the energy deposition estimates by FLUKA, we estimate that a loss rate of ~10^{11} ions/s can be sustained for a duration of 10 ms if channeling conditions are fulfilled. The allowed loss rate decreases to ~10^{10} ions/s in case the crystal is in amorphous orientation.

CONCLUSIONS

We presented for the first time an estimate of the maximum allowed fast losses for crystal collimation with a 6.8 ZTeV Pb ion beam in HL-LHC configuration based on data from fast loss events in 2023 operation. The study relies on a first benchmark of measured BLM signals against FLUKA BLM response simulations for a crystal collimator functioning in amorphous and channeling conditions. As expected, clear advantages of the latter were demonstrated.

ISBN: 978-3-95450-247-9 ISSN: 2673-5490 doi: 10.18429/JACoW-IPAC2024-TUPS39

REFERENCES

[1] J. Coupard *et al.*, "LHC Injectors Upgrade," CERN, Geneva, Switzerland, Tech. Rep. CERN-ACC-2016-0041, 2016. doi:10.17181/CERN.L6VM.UOMS

[2] O. S. Brüning *et al.*, *LHC Design Report*. CERN, 2004. doi:10.5170/CERN-2004-003-V-1

[3] R. Bruce, M. Jebramcik, J. Jowett, T. Mertens, and M. Schaumann, "Performance and luminosity models for heavy-ion operation at the CERN Large Hadron Collider," *Eur. Phys. J. Plus*, vol. 136, p. 745, 2021. doi:10.1140/epjp/s13360-021-01685-5

[4] S. Redaelli, R. Bruce, A. Lechner, and A. Mereghetti, "Chapter 5: Collimation system," pp. 87–114, 2020. doi:10.23731/CYRM-2020-0010.87

[5] G. Arduini *et al.*, "The Large Hadron Collider and the experiments for Run 3 - accelerator and experiments for LHC Run3," *JINST*, to be published.

[6] E. B. Holzer *et al.*, "Beam loss monitoring system for the LHC," in *Proc. IEEE Nuclear Science Symposium*, Puerto Rico, USA, Oct. 2005, pp. 1052–1056. doi:10.1109/NSSMIC.2005.1596433

[7] N. Fuster-Martinez *et al.*, "Simulations of heavy-ion halo collimation at the cern large hadron collider: Benchmark with measurements and cleaning performance evaluation," *Phys. Rev. Accel. Beams*, vol. 23, p. 111 002, 11 2020. doi:10.1103/PhysRevAccelBeams.23.111002

[8] S. Redaelli, "Crystal collimation of heavy ion beams," presented at IPAC'24, Nashville, TN, USA, May 2024, paper FRXN3, this conference.

[9] R. Bruce *et al.*, "HL-LHC operational scenarios for Pb-Pb and p-Pb operation," CERN, Geneva, Switzerland, Tech. Rep. CERN-ACC-2020-0011, 2020. https://cds.cern.ch/record/2722753

[10] M. D'Andrea *et al.*, "Crystal Collimation of 20 MJ Heavy-Ion Beams at the HL-LHC," in *Proc. IPAC'21*, Campinas, Brazil, May 2021, pp. 2644–2647. doi:10.18429/JACoW-IPAC2021-WEPAB023

[11] V. M. Biryukov, Y. A. Chesnokov, and V. I. Kotov, *Crystal Channeling and Its Application at High-Energy Accelerators*. Springer, Berlin, Germany, 1997. doi:10.1007/978-3-662-03407-1

[12] W. Scandale and A. Taratin, "Channeling and volume reflection of high-energy charged particles in short bent crystals. crystal assisted collimation of the accelerator beam halo," *Phys. Rep.*, vol. 815, pp. 1–107, 2019. doi:10.1016/j.physrep.2019.04.003

[13] M. D'Andrea *et al.*, "Operational performance of crystal collimation with 6.37 *Z* tev pb ion beams at the lhc," *Phys. Rev. Accel. Beams*, vol. 27, p. 011 002, 1 2024. doi:10.1103/PhysRevAccelBeams.27.011002

[14] J.-B. Potoine *et al.*, "Benchmarks of energy deposition studies for heavy-ion collimation losses at the LHC," en, *Proceedings of the 13th International Particle Accelerator Conference*, vol. IPAC2022, Thailand, 2022. doi:10.18429/JACOW-IPAC2022-WEPOST019

[15] J. Potoine *et al.*, "Power deposition studies for standard and crystal-assisted heavy ion collimation in the CERN Large Hadron Collider," *Phys. Rev. Accel. Beams*, vol. 26, no. 9, p. 093 001, 2023. doi:10.1103/physrevaccelbeams.26.093001

[16] V. Rodin *et al.*, "Evaluation of power deposition in hl-lhc with crystal-assisted heavy ion collimation," en, 2024. doi:10.18429/JACOW-HB2023-WEC2C1

[17] N. Triantafyllou, R. Bruce, and S. Redaelli, "Analysis of the performance in the 2023 LHC Pb-Pb run," presented at IPAC'24, Nashville, TN, USA, May 2024, paper TUBD2, this conference.

[18] *Fluka*, https://fluka.cern/.

[19] C. Ahdida *et al.*, "New Capabilities of the FLUKA Multi-Purpose Code," *Front. Phys.*, vol. 9, p. 788 253, 2022. doi:10.3389/fphy.2021.788253

[20] A. Mereghetti *et al.*, "Sixtrack-Fluka Active Coupling for the Upgrade of the SPS Scrapers," *Conf. Proc.*, vol. C130512, WEPEA064, 2013. https://cds.cern.ch/record/1636191

[21] *SixTrack*. http://sixtrack.web.cern.ch/SixTrack/

[22] R. De Maria *et al.*, "Sixtrack version 5: Status and new developments," en, *Proceedings of the 10th Int. Particle Accelerator Conf.*, vol. IPAC2019, Australia, 2019. doi:10.18429/JACOW-IPAC2019-WEPTS043

[23] E. Skordis *et al.*, "FLUKA coupling to Sixtrack," *CERN Yellow Rep. Conf. Proc.*, vol. 2, pp. 17–25, 2020. doi:10.23732/CYRCP-2018-002.17

[24] R. Cai, "Studies of crystal collimation for heavy ion operation at the LHC," 2024, Presented 02 May 2024. https://cds.cern.ch/record/2896673

[25] R. Cai *et al.*, "Simulation of Heavy-Ion Beam Losses with Crystal Collimation," in *Proc. IPAC'22*, Bangkok, Thailand, 2022, pp. 2082–2086. doi:10.18429/JACoW-IPAC2022-WEPOTK018

[26] E. Skordis *et al.*, "Study of the 2015 top energy LHC collimation quench tests through an advanced simulation chain," en, *Proceedings of the 8th Int. Particle Accelerator Conf.*, vol. IPAC2017, Denmark, 2017. doi:10.18429/JACOW-IPAC2017-MOPAB012

[27] B. Auchmann *et al.*, "Testing beam-induced quench levels of LHC superconducting magnets," *Physical Review Special Topics - Accelerators and Beams*, vol. 18, no. 6, p. 061 002, 2015. doi:10.1103/physrevstab.18.061002

[28] L. Bottura, M. Breschi, E. Felcini, and A. Lechner, "Stability modeling of the lhc nb-ti rutherford cables subjected to beam losses," *Phys. Rev. Accel. Beams*, vol. 22, p. 041 002, 4 2019. doi:10.1103/PhysRevAccelBeams.22.041002

[29] A. Lechner *et al.*, "Beam Loss Measurements for Recurring Fast Loss Events During 2017 LHC Operation Possibly Caused by Macroparticles," in *Proc. IPAC'18*, Vancouver, Canada, Apr.-May 2018, pp. 780–783. doi:10.18429/JACoW-IPAC2018-TUPAF040